Available online at www.sciencedirect.com

ScienceDirect

Procedia CIRP 117 (2023) 44–49

www.elsevier.com/locate/procedia

19th CIRP Conference on Modeling of Machining Operations

Digital Twin for Final Generated Surface Dimensional Error Analysis at Tool Path Level in Contour Milling

J. Rosado[a,*], P.X. Aristimuño[a], P.J. Arrazola[a]

[a] *Mondragon Unibertsitatea, Faculty of Engineering, Loramendi 4, Arrasate-Mondragón, 20500, Spain*

* Corresponding author. Tel.: +34 943 79 47 00; fax: +34 943 79 15 36. *E-mail address:* jrosado@mondragon.edu

Abstract

Surface errors in contour milling due to force induced tool deflections have a direct impact on the dimensional and geometrical accuracy of the finished part. In this sense, virtual manufacturing systems provide the capability to predict the errors generated at the final surface aiming to reduce production ramp-ups. Effects of working conditions on the surface error imprinted by the tool during a stable milling process along the whole tool path are studied at different radial and axial depths of cut. The developed process model was validated experimentally, showing good agreement in the prediction of the resulting dimensional surface error for when a single tooth is involved in the cut.

Keywords: Digital twin; Quality assurance; Accuracy; Tool path; Virtual machining

1. Introduction

Contour milling is a widely employed machining process to get mechanical components into the required specifications. That is why quality attributes of the finished surface are key performance indicators of process's efficiency. Achieving the highest possible efficiency is the main goal when adding value for manufacturing industries worldwide. In this sense, the prediction of the of the shape of the machined surface aids to proper select process parameters as well as to increase the efficiency of the machining process without introducing significant quality errors before going to the shop floor. In this sense, the collaboration between the digital and physical assets is a pivotal enabler to increase productivity and ensure quality, aiding engineers in the development and design stages of product industrialization through the increase in production know-how.

The periodical nature of the milling forces makes the tool to deflect and experience both static and dynamic distortions, which are then imprinted as dimensional errors. Forecasting the errors imprinted on the finished surface depends on the cutting parameters, machine tool, machined part and the tool itself.

The mechanics of milling processes have long been studied for the prediction of cutting forces and the resulting errors on the machined surface. Tlusty and McNeil [1] formulated the milling forces in which they demonstrated the variation of the forces in function of the angular position of the tool. Kline et al [2] predicted tool deflections and the resultant feature error, based on cantilevered beam theory. While Budak and Altintas [3] analyzed the milling forces and modelled cutter deflection, as well as proposed [4] an analytical cutting force and surface generation model in peripheral milling of very flexible, cantilevered plates with slender end mills. Smith and Tlusty [5] analyzed the different models for analysis and prediction of quality in machining operations. Seo and Cho [6] focused on flat-end milling where they considered tool deflection effects to predict the milled surface.

In contour milling, surface errors are not constant along the milled surface, they vary along the axial axis of the end mill, as Wang and Chang [7] remarked. Desai and Rao [8] also noted

10.1016/j.procir.2023.03.009

that the change in shape along the milled surface can be according to different parameters, such as, the tool geometry, cutting conditions or even cutting strategy. Islam et al. [9] modelled the end mill with an elastic beam model and considered the tool stiffness variation alongside with the static surface error prediction.

Surface error prediction also includes the dynamic aspects of the milling process, in which Schmitz and Mann [10] computed the dynamic surface location error at the tool tip, whereas Schmitz et al [11] also analyzed the impact of tool run-out on surface errors. Morelli et al [12] considered tool dynamic stiffness variation to predict the surface location error.

However, the extrapolation of the previous named analyses to the whole tool path is still a challenge. The analysis at tool path level brings plenty benefits, especially in process planning stages. This has even lead into commercially available verification software [13]. But, despite the fact these developments include analysis of the process behavior through the whole tool path, quality issues still have not gathered enough attention.

This research aims to describe the method employed to create a digital process twin and analyze the imprinted error on a machined wall through 2.5 dimensions contour milling in different machining scenarios. For this purpose, the tool path is going to be discretized and the engagement between the tool and the workpiece analyzed at each scenario change, to get the forces that take place at every tool rotation period. What is more, the influence of both radial and axial depth of cut is going to be analyzed as well as the teeth involved simultaneously in the cut.

2. Tool path discretization model

Recreating the milling process into the virtual environment requires the identification of the portion of the tool that is in direct contact with the workpiece at each pace the tool progresses along the tool path. This is the baseline for determining the instantaneous chip shape and thickness each tooth is cutting, to subsequently determine the cutting forces and the deflection of the tool.

Early process planning stages in machining include the generation of the tool path of a milling sequence in a CAM package. Nevertheless, the tool is a set of cutting edges that rotate altogether following a commanded tool path. It is for this reason that the tool path needs to be discretized in function of the portion of the workpiece the tool is touching at each position of the trajectory.

In this work, SIEMENS NX commercial CAM software has been used to generate and discretize the tool path into frames. These frames account for the intervals in which the immersion of the tool (i.e., radial depth of cut) into the workpiece vary along the tool path. For this purpose, the approximation followed to recreate the tool path will be the “circular tool path” assumption. This approach is valid as the linear advance of the tool compared to its rotational movement is rather small, so the tool path can be approximated as a series of circles [14].

The tool path discretization method works taking advantage of the material removal rate (MRR) data extracted from the CAM system while the tool is running across the tool path. This means that, while generating the tool path, the feed and the radial depth of cut will be adjusted to maintain a constant material removal rate. This variation is fundamental for determining the change on immersion and subsequently the immersion angles in which each flute enters and exits the cutting region. Figure 1 depicts an example on tool path discretization in different frames.

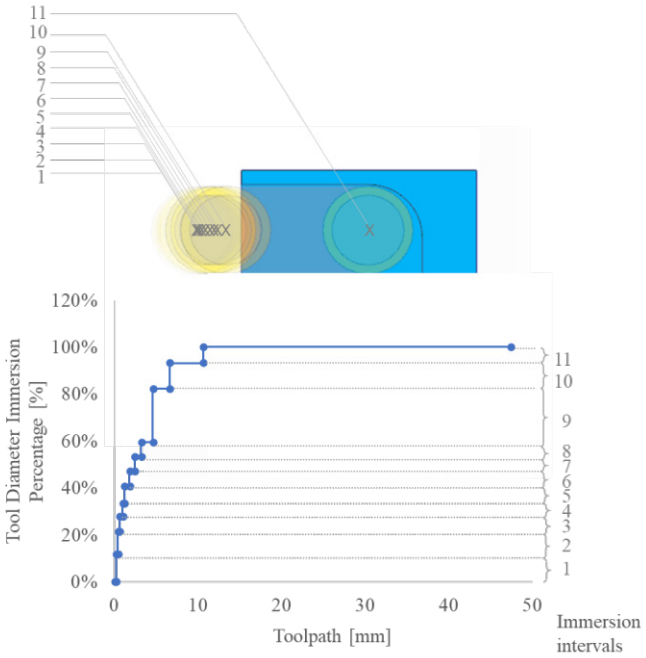

Figure 1. Tool path discretization into frames.

To finally determine the cutting region, it is necessary to classify the scenario in which the tool is going to be positioned on each interval the tool path is discretized. This information is also given by the CAM package as the instantaneous feed rate. Taking as a reference the programmed values of the tool path sequence, it could be easily determined whether the tool is (1) slotting, (2) entering in the cutting region to side mill, (3) cutting the programmed depth of cut, (4) finishing the cut, or (5) exiting the cutting region.

An *ad-hoc* post-processor has been developed to extract all this information from SIEMENS NX. The subsequent data treatment is programmed within MATLAB software.

3. Surface generation model due to static tool deflection

Once the tool path is discretized and the cutting region at each frame identified, cutting forces can be assessed. Whenever each tooth gets into the cutting region, forces are derived. While the tool rotates, the direction as well as the magnitude of these forces vary, since forces are dependent on the uncut chip load of the tool-workpiece engagement area. It is for this reason that the tool rotation needs also to be angularly split up at every frame the tool path has been discretized. This way, a series of angular steps ($\delta\phi$) will be defined and, at each angular rotation of the tool, the contribution of each tooth to the forces excerpted.

Also, as the shape of end mill edges is usually helical, the axial section of the tool that is engaged in the cut varies at every

tool rotation ($\delta\phi$). Meaning that there will be an angular delay when a portion of the tooth enters into the cut and then the subsequent portions enter in the cut in the axial direction. This is why the axial depth of cut of the tool needs also to be sectioned in infinitesimal slices perpendicular to the axial axis, so as to consider each slice as if it was a straight end mill. Therefore, a relationship is established between the helix angle (β), the angular steps ($\delta\phi$) and the diameter of the tool ($\emptyset_{Tool}$) in equation 1[10]:

$$\delta a_p = \frac{\emptyset_{Tool}/2 \cdot \delta\phi \cdot \pi/180}{\tan\beta} \tag{1}$$

The elemental tangential and radial cutting forces acting on the engaged tooth at each slice will be expressed as a function of the uncut chip load $h(\phi)$, the infinitesimal depth of cut δa_p of each disk, the cutting force coefficients contributed by the shearing action in the tangential and radial directions (K_{tc}, K_{rc}) and the edge constants (K_{te}, K_{re}) [15]:

$$\begin{aligned} \delta F_t(\phi) &= K_{tc}\delta a_p h(\phi) + K_{te}\delta a_p \\ \delta F_r(\phi) &= K_{rc}\delta a_p h(\phi) + K_{re}\delta a_p \end{aligned} \tag{2}$$

The forces acting on each tooth at each axial slice can then be projected on the feed *(x)* and cross-feed *(y)* directions in function of the instantaneous immersion angle each tooth has with respect to the reference tool axis (ϕ). The deflection of the tool is mainly going to be influenced by the forces in the cross-feed direction (F_y). Forces in other directions are going to be neglected.

The tool is going to be considered as a cantilevered beam attached to the toolholder. This is also the most flexible part of the system, since the aspect ratio of the system (diameter / length) is small. Considering the axial slices in which the tool has been sectioned, the deflection of the tool, δ_y, at a disk *k* due to the force applied at disk *m* will be computed as [16]:

$$\delta_y(z_k, m) = \begin{cases} \frac{\delta F_{y,m} v_k^2}{6EI}(3v_m - v_k), 0 < v_k < v_m \\ \frac{\delta F_{y,m} v_m^2}{6EI}(3v_k - v_m), v_m < v_k \end{cases} \tag{3}$$

where *E* refers to the Young's Modulus of the tool, *I* to the area moment of inertia considering the tool as a cylinder, v_m is the distance between the tip of the toolholder and the slice where the force is applied. And v_k the distance between the tip of the toolholder and the disk *k* where the deflection is calculated due to the applied force at disk *m* (See Figure 2).

Finally, the total static deflection at each axial slice will correspond to the addition of all deflections at that analyzed disk *k* caused by the forces at the rest of the disks [3]:

$$\delta_y(k) = \sum_{m=0}^{M} \delta_y(z_k, m) \tag{4}$$

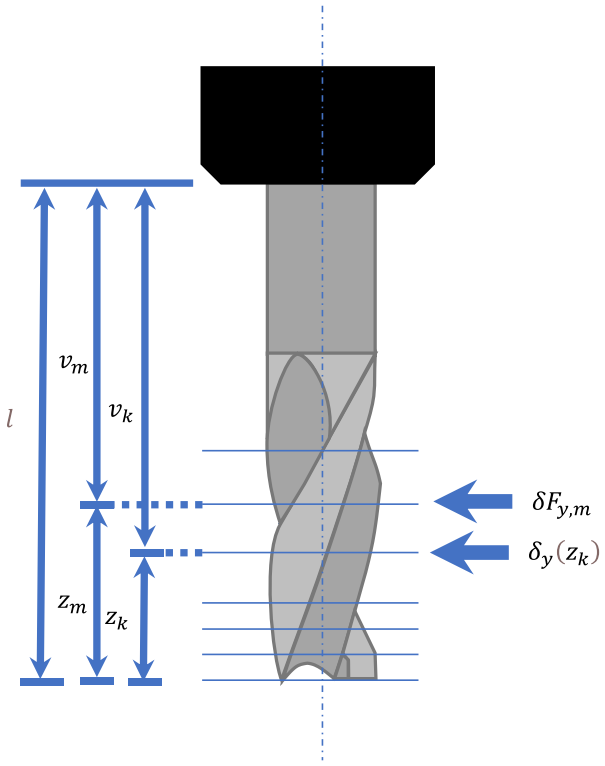

Figure 2. Tool deflection at every slice of a cantilever beam. [3]

For every angular position of the tool ($\delta\phi$), there is an axial point in which the deflection of the tool is imprinted on the machined surface. This axial points correspond to slices in which the tool is axially sectioned [16]:

$$\phi + (j-1)\phi_p - \frac{2\tan\beta}{\emptyset_{Tool}} z = \\ = \begin{cases} 0\ for\ \text{up} - \text{milling} \\ \pi\ for\ \text{down milling} \end{cases} \tag{5}$$

where ϕ is the instantaneous immersion angle, *j* the analyzed tooth, ϕ_p the pitch angle of the tool and *z* the height corresponding to the axial slice in which the deflection is calculated.

Once the profile of the dimensional error along the axial depth of cut has been deduced, the fundamental point of this research work is the extrapolation of the obtained surface profile along the whole tool path.

Despite the fact forces are going to arise whenever each portion of the teeth is immersed into the cutting region, the surface is only going to be generated in a small portion of the angular rotation of the tool ($\delta\phi$) whenever the cutting edge passes through the final surface generating zone.

Additionally, as the tooth in contact is also going to be determined by the angular position ($\delta\phi$) of the tool along the tool path, an additional assumption needs to be made: the reference tooth is going to be positioned vertically, at immersion angle 0º, when the tool starts generating the machined surface (see Figure 3). In consequence, considering the programmed feed per tooth (f_z) and the rotational speed of the tool, every tooth position can be angularly determined for

every linear displacement on the tool path, and the teeth involved in the generation of the final surface as well.

As circular tool path is assumed, the determination of the final generating surface region depends on both the diameter of the cutting tool ($\emptyset_{Tool}$) and the programmed feed per tooth (f_z) as pictured in Figure 3.

The rotation interval ($\delta\phi$) at which the edge of an analyzed tooth falls into the final generated surface zone, will actually generate the machined surface.

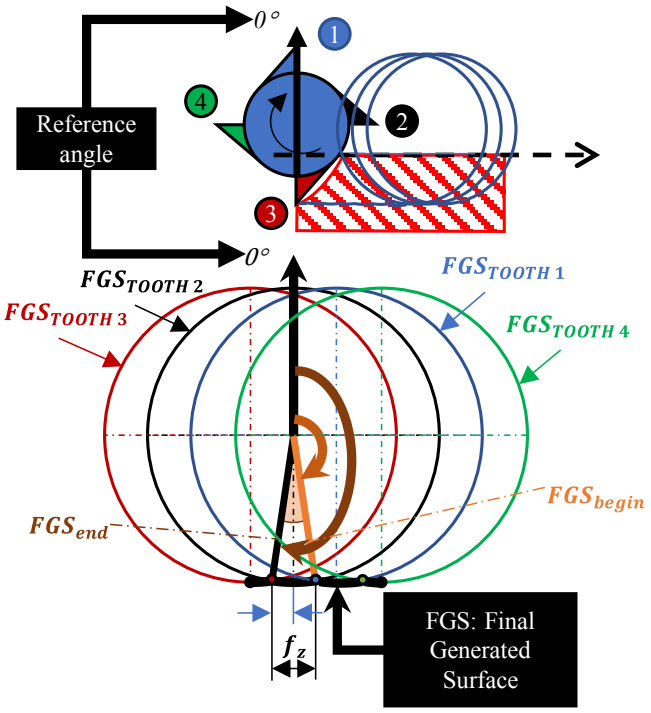

Figure 3. Final Generated Surface (FGS) on a circular tool path.

4. Experimental validation

A series of experiments have been designed to test and validate the proposed approach. The main purpose is to recreate the different scenarios the tool may encounter along a tool path in 2.5 dimensions.

As the error imprinted by the deflection of the tool is going to be the main subject of analysis, the workpiece is going to be considered as a rigid body. It is for this reason, that the suggested set up consists of a fixture mounted above a dynamometer that retains the workpiece in the cross-feed *(y)* direction mainly. Figure 4 details the disposition of the different elements used on the experiments.

The selected toolholder is a shrink fit chuck for the mechanical system to be the simplest between the spindle and the beginning of the cantilevered tool. As for the tool, the selected one will be a 4 fluted, uncoated carbide end mill of diameter 10 mm with an overall length of 72 mm provided by KENDU [17].

A number of preforms have been prepared for each experiment to sample different machining scenarios along the tool path. Each preform has different steps that emulate different immersions of the tool as it moves across the commanded tool path. Figure 5 depicts graphically the geometry of the specimen. Each preform consists of five sections (every section has a different radial depth of cut, a_e) at a fixed axial depth of cut (a_p). Section 0 will act as a pre-charge segment. Thus, the radial depth of cut of this section (a_e0) will be very small. This way, the machined surface on this section will act as the reference surface for dimensional measurement purposes on the rest of sections. The configuration of the remaining sections, as well as the axial depth of cut (a_p) of the specimen will depend on the desired number of teeth to be involved in the cut at each section.

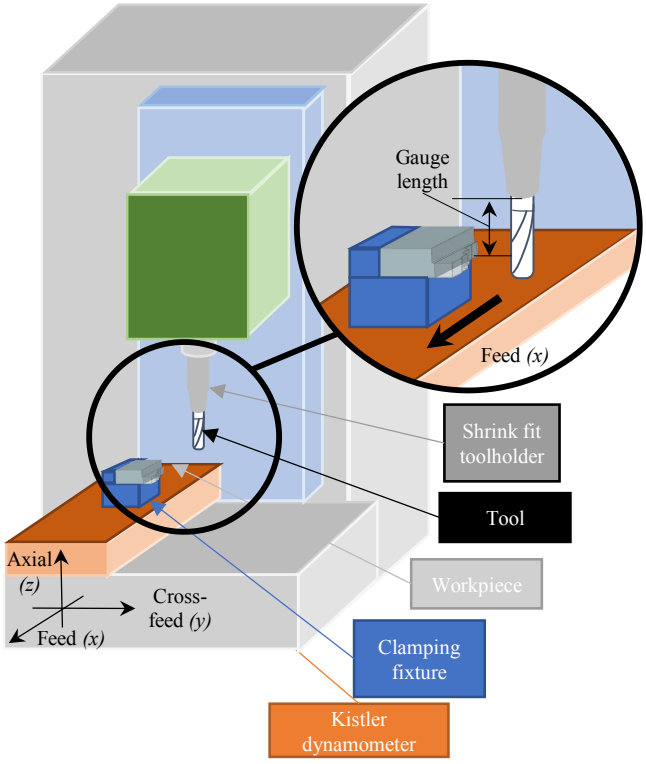

Figure 4. Experimental set up.

The more the teeth involved simultaneously in the cut, the higher the cutting forces are expected to be. Thus, a higher tool deflection ought to be achieved. Thereby, as pictured in Figure 5, immersions (radial depth of cut for each section, a_e) are going to be set up so as one tooth gets involved in the cut in the sections 1 and 2, and the second teeth is expected to get into the cut simultaneously as long as the tool moves forward the tool path and gets into sections 3 and 4. The axial depth of cut (a_p) projected for each preform also plays an important role, as the bigger the axial depth of cut (a_p), the highest the contribution of each tooth to the cut will be, expecting higher deflections as well as higher vibrations.

Another variable to get into consideration is the stiffness of the whole system as well as the cantilever gauge length left when machining, this being the distance between the tip of the toolholder and the bottom of the machined surface, as specified in Figure 4.

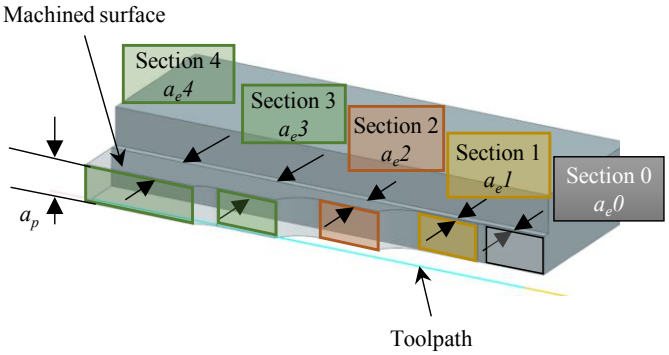

Figure 5 Geometrical shape of each specimen.

Table 1 shows the different design and process conditions projected for the different specimens.

Table 1. Experiment details.

Specimen	Specimen design parameters						Process conditions	
	a_p [mm]	a_e0 [mm]	a_e1 [mm]	a_e2 [mm]	a_e3 [mm]	a_e4 [mm]	v_c [m/min]	f_z [mm/tooth]
1	3	0.1	0.3	2.5	5.43	6.29	150	0.125
2	4	0.1	0.3	2.5	5.43	6.29	150	0.125
3	5	0.1	0.3	2.5	5.43	6.29	150	0.125

The selected material for the experiments has been a low carbon steel: AISI 1045. Which, from independent cutting tests [18], the cutting coefficients are determined to be K_t = 1730 N/mm^2, K_n = 723 N/mm^2, K_{te} = 4 N/mm and K_{ne} = 26 N/mm.

As remarked, test conditions have been conducted at v_c = 150 m/min and f_z = 0.125 mm/tooth. Every test has followed a down milling strategy and the cantilever gauge distance left from the tip of the toolholder to the bottom of the machined wall is 20 mm.

After conducting the experiments, KEYENCE LK-G30 laser has been used for measuring the machined surface. The laser has been mounted on the machine tool itself and every section has been scanned at three vertical passes per section. Data has been captured at a frequency of 250 Hz and at a feed of 50 mm/min.

5. Result discussion

The results shown on the boxplot chart in Figure 6 depict the distribution the surface error has along the axial axis of the machined surface. Box limits indicate the range of the central 50% of the data and the results are plotted regarding every section, specified in Figure 5. Statically tool deflection predicted results by the digital model are first plotted, in red color, on the left side of each result pair, while the obtained ones in the experiments by laser measurements are plotted on the right side, blue colored.

Results show a good agreement for those sections in which the immersion is rather small and, consequently, only one tooth is actually cutting (e.g., section 1 and section 2). As for location, the surface error goes in accordance with what has been predicted in these two sections as the median lines lie within the box lengths. Additionally, box lengths denote that the dispersion of the surface error generated by one tooth is kept between the measured limits, achieving an error rate below the thirty percent. Consequently, results are acceptable for predicting the static surface errors by the virtual machining model when one tooth is engaged into the cut.

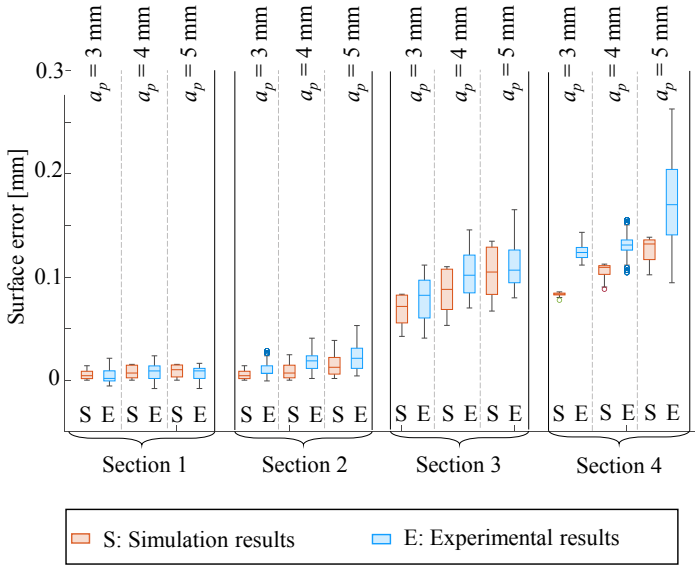

Figure 6. Experimental and simulation results.

However, differences arise when a second tooth gets involved in the cut. As expected, deflection values increase due to the effect the second tooth has on the forces and subsequently, on the deflection produced by the forces.

At section 3, where the second tooth is bound to get engaged into the cut in all the cases, result location agreement is well maintained for different depths of cut. However, the dispersion of the results exhibits differences between the predicted and the actual measurement. Results are not kept in between the limits of the boxes nor the differences between the whiskers is kept between acceptable ranges.

Finally, at section 4, where the immersion is bigger, differences are notable. The jump on immersion in this case from the previous section 3, is of 10 degrees. Compared to the jumps in immersion between section 1 and section 2 (40 degrees) and between sections 2 and 3 (35 degrees), it is the smallest jump, and this is reflected on the predicted results. In contrast, measured results show a big difference from what is predicted. This difference has its roots on the fact that the digital model has been built considering the static deflection feedback model of the tool. But, in reality, as a tooth passes the surface left by the previous teeth needs also to be considered, as this affects to the force exerted by the current tooth and thus, to the deflection. Consequently, further research considering the dynamics of the process ought to be considered.

6. Summary and outlook

This research work presents a virtual model predicting tool deflections and, thus geometrical and dimensional surface errors on the imprinted surface during end milling. The main conclusions of this research work are:

- Static tool deflection predictions have shown a good agreement for determining the error imprinted on the milled surface for the cases in which only one tooth is cutting simultaneously. For the cases where more teeth get into the cut simultaneously, meaning a bigger radial depth of cut, the agreement is not good enough.
- As for the axial depth of cut, a decrease on the effects of vibrations has been observed as the machined surface has been axially decreased and chatter marks disappeared for small radial depths of cut as well. Also, it has been observed there is an angle from which the same length of the cutting edge will be engaged in the cut, regardless of the radial depth of cut. Thus, constant cutting forces are achieved from that angle until the second tooth is engaged into the cut simultaneously. This effect is shown for both simulation and experimental results in Figure 6 in sections 1 and 2 at a_p = 3 mm.
- The intermittent nature of the cutting forces will always cause the tool to vibrate. Even if there is no chatter, the angular position of the teeth in the vibration cycle of the tool as they generate the final machined surface will contribute to determine the location of the machined surface. This phenomenon needs to be further studied as process dynamics go beyond the static surface errors.

Acknowledgements

The authors thank OPTICED (KK-2021/00003) project for the financial support given to develop this work.

References

[1] J. Tlusty, and P. McNeil, ‘Dynamics of Cutting Forces in End Milling.’, *Annals of CIRP*, vol. 24/1, pp. 21–25, 1975.

[2] W. A. Kline, R. E. DeVor, and J. R. Lindberg, ‘The prediction of cutting forces in end milling with application to cornering cuts’, *International Journal of Machine Tool Design and Research*, vol. 22, no. 1, pp. 7–22, Jan. 1982, doi: 10.1016/0020-7357(82)90016-6.

[3] E. Budak and Y. Altintas, ‘Peripheral milling conditions for improved dimensional accuracy’, *International Journal of Machine Tools and Manufacture*, vol. 34, no. 7, pp. 907–918, Oct. 1994, doi: 10.1016/0890-6955(94)90024-8.

[4] E. Budak and Y. Altintas, ‘Modeling and avoidance of static form errors in peripheral milling of plates’, *International Journal of Machine Tools and Manufacture*, vol. 35, no. 3, pp. 459–476, Mar. 1995, doi: 10.1016/0890-6955(94)P2628-S.

[5] S. Smith and J. Tlusty, ‘An Overview of Modeling and Simulation of the Milling Process’, *ASME Digital Collection*, 1991.

[6] T.-L. Seo and M.-W. Cho, ‘Tool Trajectory Generation Based on Tool Deflection Effects in the Flat-End Milling Process (ll) -Prediction and Compensation of Milled Surface Errors-’, p. 13.

[7] M.-Y. Wang and H.-Y. Chang, ‘A simulation shape error for end milling AL6061-T6’, *The International Journal of Advanced Manufacturing Technology*, vol. 22, no. 9–10, pp. 689–696, Nov. 2003, doi: 10.1007/s00170-003-1570-9.

[8] K. A. Desai and P. V. M. Rao, ‘On cutter deflection surface errors in peripheral milling’, *Journal of Materials Processing Technology*, vol. 212, no. 11, pp. 2443–2454, Nov. 2012, doi: 10.1016/j.jmatprotec.2012.07.003.

[9] M. N. Islam, H. U. Lee, and D.-W. Cho, ‘Prediction and analysis of size tolerances achievable in peripheral end milling’, *Int J Adv Manuf Technol*, p. 13, 2008.

[10] T. Schmitz and B. Mann, ‘Closed-form solutions for surface location error in milling’, *International Journal of Machine Tools & Manufacture*, 2006.

[11] T. L. Schmitz, J. Couey, E. Marsh, N. Mauntler, and D. Hughes, ‘Runout effects in milling: Surface finish, surface location error, and stability’, *International Journal of Machine Tools and Manufacture*, vol. 47, no. 5, pp. 841–851, Apr. 2007, doi: 10.1016/j.ijmachtools.2006.06.014.

[12] L. Morelli, N. Grossi, G. Campatelli, and A. Scippa, ‘Surface location error prediction in 2.5-axis peripheral milling considering tool dynamic stiffness variation’, *Precision Engineering*, vol. 76, pp. 95–109, Jul. 2022, doi: 10.1016/j.precisioneng.2022.03.008.

[13] T. Marusich, S. Usui, L. Zamorano, K. Marusich, and Y. Oohnishi, ‘Improved Titanium Machining: Modeling and Analysis of 5-Axis Toolpaths via Physics-Based Methods’, *Proceedings of 4th CIRP International Conference on High Performance Cutting*, 2010.

[14] T. L. Schmitz and K. S. Smith, *Machining Dynamics*. Boston, MA: Springer US, 2009. doi: 10.1007/978-0-387-09645-2.

[15] Y. Altintas, A. Spence, and J. Tlusty, ‘End Milling Force Algorithms for CAD Systems’, *CIRP Annals*, vol. 40, no. 1, pp. 31–34, 1991, doi: 10.1016/S0007-8506(07)61927-1.

[16] Y. Altintas, *Manufacturing Automation: Metal Cutting Mechanics, Machine tool Vibrations, and CNC Design*, 2nd ed. Cambridge: Cambridge University Press, 2011. doi: 10.1017/CBO9780511843723.

[17] KENDU Cutting Tools, ‘KENDU Cutting Tools Catalogue’. [Online]. Available: https://www.kendu.es/en/catalogues/

[18] O. Gonzalo, J. Beristain, H. Jauregi, and C. Sanz, ‘A method for the identification of the specific force coefficients for mechanistic milling simulation’, *International Journal of Machine Tools and Manufacture*, vol. 50, no. 9, pp. 765–774, Sep. 2010, doi: 10.1016/j.ijmachtools.2010.05.009.